



Comparison of Tropical Cyclone Wind Radius Estimates between the KMA, RSMC Tokyo, and JTWC

Hye-Ji Kim¹ · Il-Ju Moon¹ · Imyong Oh²

Received: 23 November 2021 / Revised: 4 February 2022 / Accepted: 6 February 2022 / Published online: 4 April 2022
© The Author(s) 2022

Abstract

This study compared estimates of gale-force wind radii (R30 or R34) and storm-force wind radii (R50) of tropical cyclones (TC) by three agencies—the Korea Meteorological Administration (KMA), the Regional Specialized Meteorological Center (RSMC) Tokyo, and the Joint Typhoon Warning Center (JTWC)—in the western North Pacific during 2015–2018 and investigated the characteristics of these estimates. The results showed that the KMA's R30 and R50 estimates were smaller (38% and 29%, respectively) than those of the RSMC Tokyo, and larger (11%) for R30 and smaller (12%) for R50 than those of the JTWC. The differences between these agencies seem to be largely determined by whether the agency estimates wind radii based only on a TC's own winds or on TC winds combined with other mid-latitude synoptic systems to make TC warnings more comprehensive. The former is mainly the practice of the KMA and JTWC, whereas the latter is mainly the practice of the RSMC Tokyo. The factors considered for estimating wind radii also differ between the agencies: the KMA heavily relies on TC intensity—the higher the intensity, the larger the radius—while the RSMC Tokyo and JTWC rely less on TC intensity than the KMA but additionally consider the latitude and storm translation speed in their estimations. In particular, the TC translation speed considered by the RSMC Tokyo and JTWC explains why their estimated wind radii exhibit, on average, greater asymmetries (i.e., greater differences between the longest and shortest radii) than those estimated by the KMA. The findings of agency-dependent characteristics of TC wind radius data help to better determining and understanding the TC impact areas for TC risk reduction and management.

Keywords Tropical cyclone · Gale-force wind radii · Storm-force wind radii · Three agencies

1 Introduction

The size of a tropical cyclone (TC), which is directly related to the extent of its damage area, is important information that global TC warning centers provide as part of their TC advisory and warning processes. Global TC warning centers estimate the TC size based on the maximum radial extent of critical wind speed thresholds, such as 30-, 34-, and 50-kt

wind radii, from the storm center (hereafter R30, R34, R50, respectively). The TC size is mainly used for wind-based risk and impact assessments, as well as wave and surge forecasting (Knaff et al. 2017). However, studies on the TC size have received little attention compared to studies using other metrics, such as TC track and intensity, despite the importance of the TC size in operational forecasts (Chavas et al. 2015). This is partly because the TC size is usually estimated in a subjective way, which reduces the accuracy and consistency of the data (Landsea and Franklin 2013; Knaff et al. 2017; Cha et al. 2020), making the study of the TC size difficult. Indeed, although global TC warning centers make significant efforts to produce accurate TC size data, they exhibit significant differences between them (Song and Klotzbach 2016).

In general, TC wind radii are estimated based on available information using numerical models, statistical wind radius climatology and persistence (CLIPER) models, and satellite-derived data from various operational agencies

Responsible Editor: Dong-Hyun Cha

✉ Il-Ju Moon
ijmoon@jejunu.ac.kr

¹ Typhoon Research Center/ Graduate School of Interdisciplinary Program in Marine Meteorology, Jeju National University, 102 Jejudaehak-ro, Jeju 632-43, South Korea

² National Typhoon Center, Korea Meteorological Administration, Jeju, South Korea

(McAdie 2004; Sampson and Knaff 2015; Knaff et al. 2016). In particular, satellite winds are primary observation sources for estimating the wind radius by agencies instead of aircraft reconnaissance and surface observations that are not routinely available (Brennan et al. 2009). In U.S. TC warning centers, namely the National Hurricane Center, the Central Pacific Hurricane Center (NHC), and the Joint Typhoon Warning Center (JTWC), numerous scatterometers such as Quick scatterometer (Lungu and Callahan 2006), WindSat, Oceansat-2, Advanced Scatterometer (ASCAT) (Bentamy et al. 2008), Scatterometer Satellite (Misra et al. 2019) and more recently Haiyang-2 scatterometer (Zhao and Zhao 2019) are used to postseason subjective and objective reanalysis of wind radii (Sampson et al. 2017, 2018; Knaff et al. 2021). In the Regional Specialized Meteorological Center (RSMC) Tokyo, TC parameters including R30 and R50 are determined with overall available observations such as Himawari-8 satellite images, Radar, surface synoptic observations, ship, buoy, and ASCAT. In the absence of necessary observations, the RSMC Tokyo estimates R30 and R50 from regression equation between central pressure and wind radius (Muroi 2018). In the Korea Meteorological Administration (KMA), the postseason analysis of wind radii is primary based on direct estimates from satellite observations such as ASCAT, Multiplatform Tropical Cyclone Surface Wind Analysis (MTCSWA) (Knaff et al. 2011), and Microwave Radiometers (Hong and Shin 2013). When these data are not available, the KMA indirectly estimates TC wind radii from the regression between wind radii and maximum wind speed (V_{max}) using the KMA infrared satellite data (Kwon 2012; Lee and Kwon 2015). As such, agencies generally use similar data in their postseason analysis to generate wind radius, but each agency has its own method of estimating TC wind radii, which results in different estimates of the same storm. For instance, Song and Klotzbach (2016) found a considerable discrepancy in wind radius estimates between the RSMC Tokyo and the JTWC due to differences in their detailed estimation techniques.

Understanding such differences in wind radius estimates among agencies is a prerequisite for performing TC size-related studies. The International Best Track Archive for Climate Stewardship (IBTrACS) has been providing TC wind radii since version 4, in which the RSMC Tokyo has provided the longest and shortest R30 and R50 for gale-force and storm-force wind radii, respectively, from 1979 to the present (Knaff et al. 2021). Meanwhile, the JTWC has provided R34 and R50 data from 2001 to the present (Lee et al. 2010). The KMA has also provided postseason reanalysis or best tracking of wind radii, which include the longest and shortest R30 and R50, since 2015 (KMA 2019). However, how the wind radius estimates of the KMA, RSMC Tokyo, and JTWC differ from each other and whether they have unique characteristics have not yet been evaluated.

The TC size is known to be related to the V_{max} , latitude, TC translation speed (TCTS), and storm age (Merrill 1984; Weatherford and Gray 1988; Bell and Ray 2004; Kimball and Mulekar 2004; Knaff et al. 2007; Kossin et al. 2007; Wu et al. 2015). Such parameters are used for the development of statistical models, such as the CLIPER model, which is one of the operational models of the NHC and the JTWC (Knaff et al. 2007). In particular, the relationship between V_{max} and R34, which show a strong positive correlation, has been widely used in operations (Weatherford and Gray 1988; Chan and Chan 2012; Song and Klotzbach 2016). Latitude is the most frequently used factor for TC size estimations after V_{max} —the higher the latitude, the larger the TC size (Merrill 1984; DeMaria and Pickle 1988). It has also been reported that fast poleward-moving TCs increase their angular momentum, which is associated with an increase in TC size, suggesting that the TC size can be affected by the TCTS as well as the latitude (Chan and Chan 2013). The latitude and TCTS are key factors affecting not only wind radii but also their asymmetries: the higher the latitude and the faster the TCTS, the greater the asymmetry (Frank and Gray 1980; Dougherty and Davis 2014; Knaff et al. 2016). Storm age is closely related to V_{max} and latitude—as storm age increases, the TC moves to higher latitudes and V_{max} tends to increase (Knaff et al. 2016), resulting in a high correlation between storm age and TC size (Kossin et al. 2007; Dolling et al. 2016; Schenkel et al. 2017). Therefore, it is important to know how each agency considers these TC size-related parameters in its wind radius estimations, as this helps to understand wind radius estimation discrepancies among agencies.

This study aimed to investigate the characteristics of R30, R34, and R50 estimated by three agencies—the KMA, RSMC Tokyo, and JTWC—including their asymmetrical characteristics in terms of V_{max} and spatial distributions. We also aimed to examine how each agency considers TC size-related factors (V_{max} , latitude, TCTS, and storm age) in its TC wind radius estimations by comparing the correlation coefficients between these factors and the TC wind radii.

The rest of this paper is organized as follows. Section 2 describes the data and methods used. Section 3 presents the results of the comparison of wind radius estimates between the three agencies. Section 4 describes how each agency considers the factors affecting the TC size. The final section summarizes the results and concludes the paper.

2 Data and Methods

RSMC Tokyo and JTWC best track data from 2015 to 2018 were obtained from IBTrACS version 4, which includes TC position, intensity, and wind radius information at 6-h intervals. KMA best track data were obtained

from the National Typhoon Center of the KMA. For a unified analysis, all wind radius data (R30, R34, and R50) were reconstructed by averaging the longest and shortest radius estimates of the KMA and RSMC Tokyo and four-quadrant wind radii (northeast, southeast, southwest, and northwest) for the JTWC based on KMA information. The R30 data were the 30-kt wind radii used by both the RSMC Tokyo and the KMA based on 10-min mean wind speeds, while the R34 data were the 34-kt wind radii used by the JTWC based on 1-min mean wind speeds. The definition difference in wind speeds between the RSMC Tokyo/KMA and the JTWC can make a direct comparison between R30 and R34 difficult. However, a sensitivity experiment that converted the data to the same wind speed definition showed that the difference had a minor effect. This may be because 34 kts in 1-min mean wind speed intervals is about 30 kts in 10-min mean wind speed intervals when a conversion factor of 1.14 is used (Barcikowska et al. 2012). Therefore, we directly compared R30 and R34 (hereafter, for convenience, the JTWC's R34 is used as R30). Meanwhile, the JTWC's R50 have been analyzed after applying the conversion factor.

The ways in which each agency considers TC size-related factors (Vmax, latitude, and TCTS) in its TC wind radius estimations were examined by comparing the correlation coefficients between these factors and the estimated TC wind radii. The results were also used to investigate the agency-dependent asymmetrical characteristics of wind radii. The TCTS was calculated using centered time differencing based on changes in latitude and longitude at 12-h intervals, except for the first and last cases, in which one-sided time differencing was used (Xu and Wang 2018). The asymmetries in wind radii were calculated as

the differences between the longest and shortest radii of the TCs divided by 2 (Song and Klotzbach 2016).

3 Results

3.1 Comparison of Wind Radius Estimates between the Three Agencies

To examine the characteristics of the TC wind radii estimated by the KMA, RSMC Tokyo, and JTWC, the correlations and mean values were first compared between the three agencies. The first observation was that the correlation coefficient (0.75–0.81) of R30 was overall higher than that of R50 (0.57–0.70). This suggests that the agencies have greater difficulty estimating TC wind radii in stronger winds due to the relatively smaller sample and few tools available for radius estimation. The KMA and RSMC Tokyo showed the strongest correlations in R30 and R50 (0.81 and 0.70, respectively; Fig. 1a, d), while the KMA and JTWC showed the weakest correlations (0.75 and 0.57, respectively; Fig. 1b, e). The RSMC Tokyo showed strong R30 and R50 correlations with the other two agencies (Fig. 1a, c, d, and f).

A comparison between the mean values of each agency showed that the RSMC Tokyo had the largest mean value (334 ± 134 km) for R30, followed by the KMA (242 ± 92 km) and the JTWC (216 ± 95 km). The mean R30 value of the RSMC Tokyo was about 91 and 117 km larger than those of the KMA and JTWC, respectively (Table 1). The KMA's mean R30 was smaller than that of the RSMC Tokyo but larger than that of the JTWC. For R50, the RSMC Tokyo also had the largest mean value (129 ± 52 km), followed by the JTWC (113 ± 45 km)

Fig. 1 Scatter plots of tropical cyclone wind radius estimates of the KMA, RSMC Tokyo, and JTWC. The top (R30) and bottom (R50) panels compare the KMA and RSMC Tokyo (a, d), the KMA and JTWC (b, e), and the RSMC Tokyo and JTWC (c, f). Correlation coefficients (r) and mean differences (MD) between the agencies are indicated in the bottom right corner of each panel. The unit of MD is km

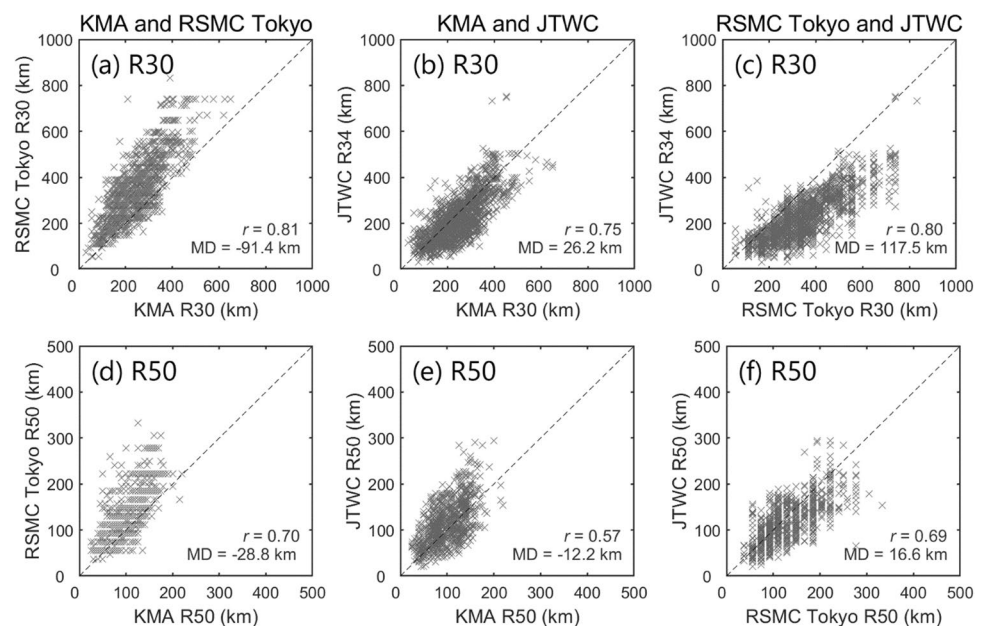


Table 1 Comparison of mean tropical cyclone wind radius values and their standard deviations between the KMA, RSMC Tokyo, and JTWC. “*N*” indicates the number of samples. The parenthetical val-

ues represent the difference between KMA and other agencies, and the ratio of the difference to the KMA value

	KMA	RSMC Tokyo	JTWC
R30 (Num = 1913)	242.3 ± 92.3 km	333.7 ± 133.6 km (−91.4 km, −38%)	216.2 ± 95.4 km (26.1 km, 11%)
R50 (Num = 1081)	100.4 ± 34.5 km	129.3 ± 51.5 km (−28.9 km, −29%)	112.7 ± 45.0 km (−12.3 km, −12%)

and the KMA (100 ± 35 km). The KMA’s mean value was about 12–29 km smaller than those of the other two agencies.

To determine the range in which differences in TC wind radii mainly appeared between the agencies, the differences were compared by dividing R30 and R50 into bins at 100- and 50-km intervals, respectively (Fig. 2). In R30, the difference between the RSMC Tokyo and JTWC showed positive values in all ranges, while the difference between the KMA and RSMC had negative values (blue and black lines, respectively, in Fig. 2a). This suggests that the RSMC Tokyo estimated larger R30 values than the JTWC and KMA in all ranges. The JTWC had larger R30 values than the KMA in wind radii of less than 100 km but smaller values than the KMA in radii of over 200 km. The absolute differences between the agencies increased as the TC wind radii increased.

In R50 (Fig. 2b), the differences both between the KMA and RSMC (black) and between the KMA and JTWC (red) had negative values except over 200 km. This suggests that the KMA estimated smaller R50 values than the RSMC Tokyo and JTWC in most ranges. The JTWC had smaller R50 values than the RSMC Tokyo except over 200 km.

Unlike R30, the absolute differences between the agencies did not change significantly as the TC wind radii increased.

To compare the spatial distributions of estimated TC wind radii between the agencies, the wind radii of all TCs occurring during the study period were averaged for the grid of $2^\circ \times 2^\circ$ using a moving window of 4° by 4° to remove outliers with large spatial variability (Fig. 3). In R30, all three agencies had larger values than average in the central region of the WNP ($120\text{--}160^\circ\text{E}$, $15\text{--}45^\circ\text{N}$) and relatively small values at low latitudes (below 15°N), the South China Sea, and the inland area of East Asia (Fig. 3a–c). The difference between the KMA and RSMC Tokyo showed negative values (Fig. 4a), while the difference between the RSMC Tokyo and JTWC showed positive values (Fig. 4c). This suggests that the RSMC Tokyo estimated larger R30 values than the JTWC and KMA in most regions. In particular, the RSMC Tokyo had larger R30 values than the other two agencies at higher latitudes. The JTWC had larger R30 values than the KMA in the inland area of China and along the coast of the Korean Peninsula but smaller R30 values than the KMA at latitudes below 20°N (Fig. 4b).

In R50, the RSMC Tokyo and JTWC showed similar spatial distributions, especially in that they have large

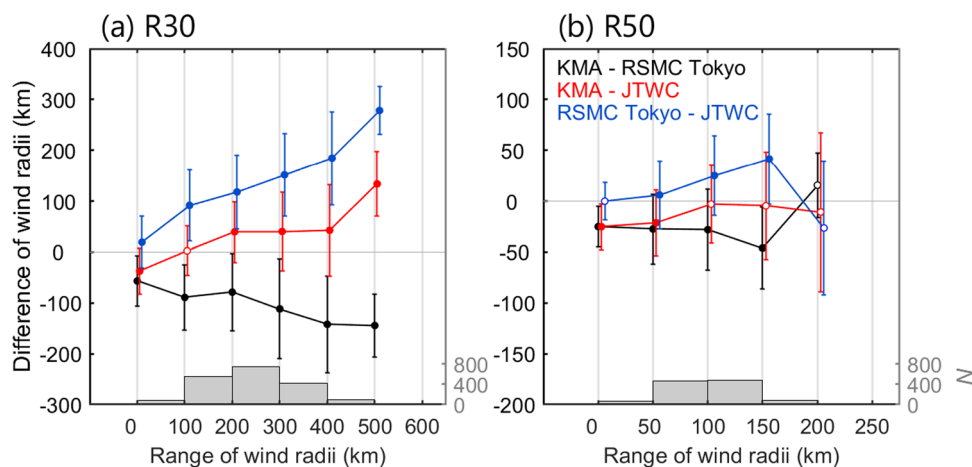


Fig. 2 Mean differences in wind radius estimates between the KMA and RSMC Tokyo (black), between the KMA and JTWC (red), and between the RSMC Tokyo and JTWC (blue) for each bin of R30 (a) and R50 (b). The bins were divided based on the tropical cyclone

wind radius estimates of the KMA. The error bars indicate standard deviations. The gray bar graph represents the numbers (*N*) of R30 and R50 samples for each bin at 100- and 50-km intervals, respectively. The filled circles indicate significant differences at the 95% level

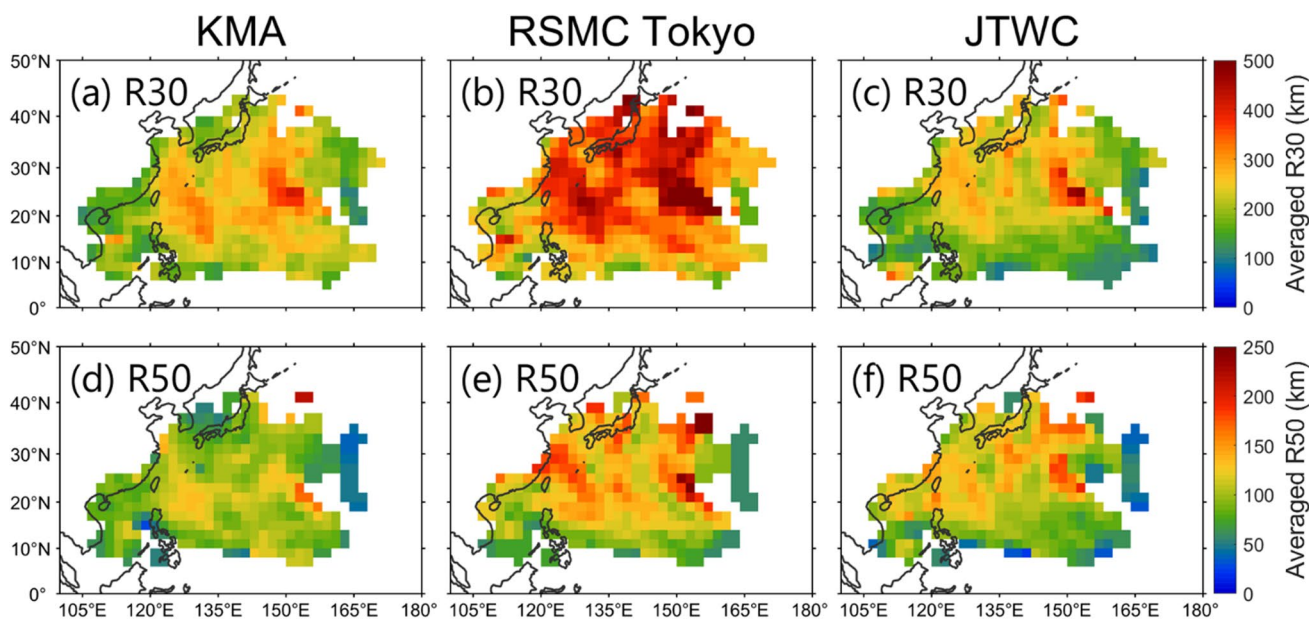


Fig. 3 Comparisons of the spatial distributions of tropical cyclone R30 (top panels) and R50 (bottom panels) between the KMA (a, d), RSMC Tokyo (b, e), and JTWC (c, f) during 2015–2018. In each grid, the values were averaged along a moving window of 4° by 4° to smooth the wind radius of each grid

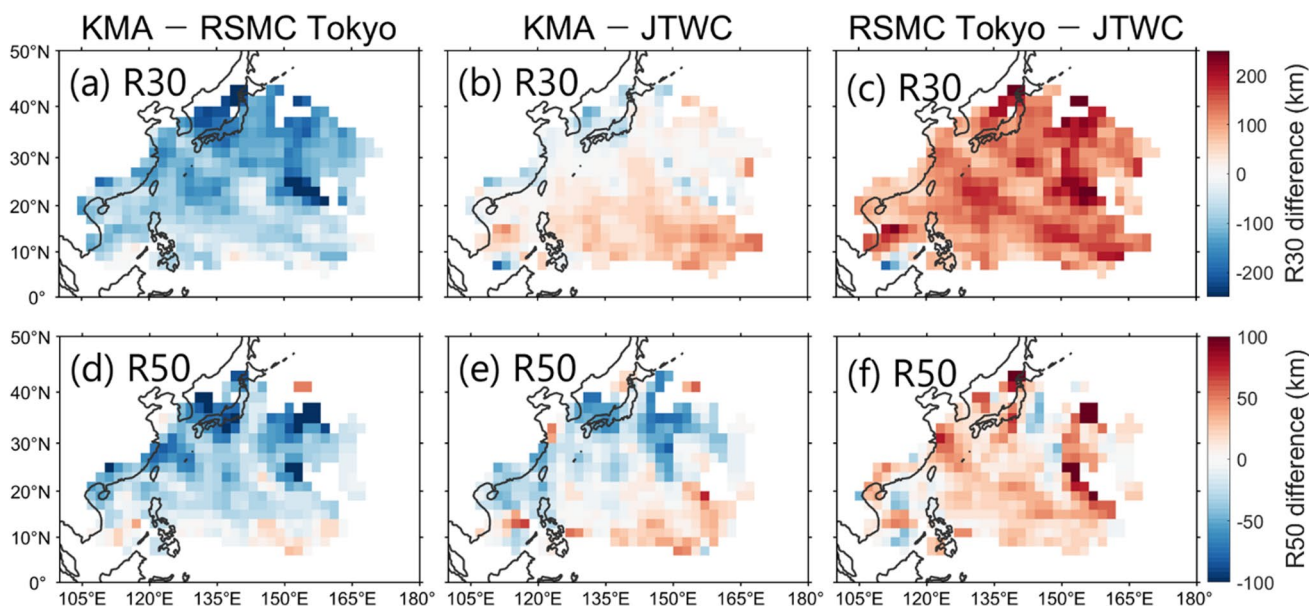


Fig. 4 Comparisons of the spatial distributions of mean differences in tropical cyclone R30 (top panels) and R50 (bottom panels) between the KMA and RSMC Tokyo (a, d), between the KMA and JTWC (b, e), and between the RSMC Tokyo and JTWC (c, f) during 2015–2018. In each grid, the values were averaged along a moving window of 4° by 4° to smooth the wind radius of each grid

values near Japan and Taiwan, but the KMA showed different distributions overall (Fig. 3d–f). The spatial differences between the agencies showed that the KMA had smaller R50 values than the RSMC Tokyo and JTWC in most regions except low latitudes below 10°N (Fig. 4d

and e). For the RSMC Tokyo and JTWC significant differences were found in the open seas east of 150°E (Fig. 4f).

3.2 Relationship between Wind Radii and Potential TC Size-Related Environmental Variables

To examine the extent to which the four key parameters related to the TC size (V_{\max} , latitude, TCTS, and storm age) affected the three agencies' estimations of TC wind radii, the correlations between the four parameters and the TC wind radii were examined (Table 2). The results showed that of the four parameters, V_{\max} had the strongest correlations with R30 and R50 overall, with stronger correlations in the KMA (0.61–0.62) estimations than in the estimations of the other two agencies (0.27–0.44). The similarity of the spatial distribution of V_{\max} to that of R30 and R50 supports the strong correlation between them (see Figs. 3 and 5a). Latitude did not correlate with wind radii in the KMA estimates (-0.04 to 0.05) but had weak correlations in the RSMC Tokyo and JTWC estimates (0.20 – 0.28). Similarly, the TCTS showed little correlation with wind radii in the KMA estimates (-0.02 to 0.06) and weak correlations in the RSMC Tokyo and JTWC estimates (0.10 – 0.19). These results indicate that the KMA mainly consider only V_{\max} when estimating TC wind radii (Lee and Kwon 2015), while the RSMC Tokyo and JTWC additionally consider the latitude and TCTS in addition to V_{\max} (Knaff et al. 2007). Meanwhile, storm age had a significant correlation with wind radii of all agencies (RSMC Tokyo, 0.35 – 0.37 ; JTWC, 0.23 – 0.41 ; KMA, 0.18 – 0.37). The high correlations can be explained by the fact that storm age is correlated with

Table 2 Pearson's correlation coefficients and their p -values between tropical cyclone wind radii (R30, R50) and tropical cyclone size-related environmental variables (maximum wind speed, latitude, TC translation speed, and storm age) for the three agencies. The units of V_{\max} , Latitude, TCTS, and Storm age are kt, °N, ms^{-1} and day, respectively

TC wind radii		Correlation coefficient		
		KMA	RSMC Tokyo	JTWC
R30	V_{\max}	0.62 ($p < 0.01$)	0.38 ($p < 0.01$)	0.44 ($p < 0.01$)
	Latitude	0.05 ($p < 0.01$)	0.24 ($p < 0.01$)	0.28 ($p < 0.01$)
	TCTS	0.06 ($p < 0.01$)	0.18 ($p < 0.01$)	0.19 ($p < 0.01$)
	Storm age	0.37 ($p < 0.01$)	0.37 ($p < 0.01$)	0.41 ($p < 0.01$)
R50	V_{\max}	0.61 ($p < 0.01$)	0.41 ($p < 0.01$)	0.27 ($p < 0.01$)
	Latitude	-0.04 ($p = 0.90$)	0.20 ($p < 0.01$)	0.24 ($p < 0.01$)
	TCTS	-0.02 ($p = 0.26$)	0.10 ($p < 0.01$)	0.17 ($p < 0.01$)
	Storm age	0.18 ($p < 0.01$)	0.35 ($p < 0.01$)	0.23 ($p < 0.01$)

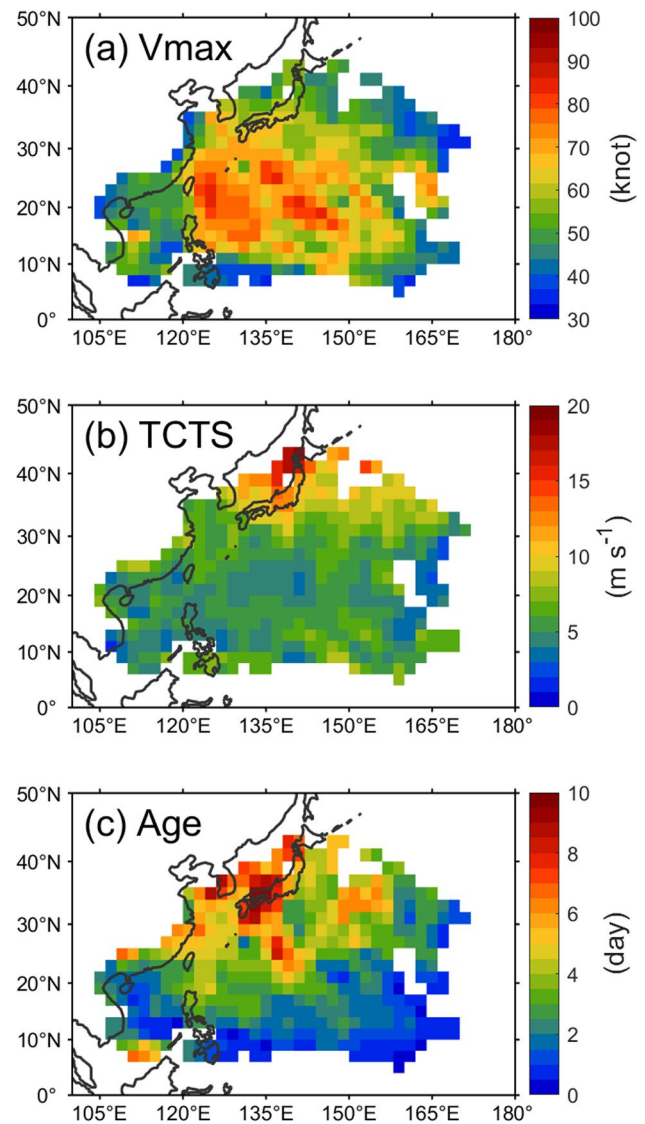


Fig. 5 Spatial distributions of maximum wind speed (V_{\max}) (a), TC translation speed (TCTS) (b), and storm age (Age) (c) based on the KMA best track data during 2015–2018. In each grid, the values were averaged along a moving window of 4° by 4° for smoothing

V_{\max} (0.34 – 0.43) and latitude (0.40 – 0.46), respectively. On the other hand, the large difference in wind radii (especially in R50) between the KMA and other agencies in the East Sea and the eastern seas of Japan (Fig. 3) seems to be due to the influence of TCTS and storm age, which have large values in the vicinity (Fig. 5b and c). This is because the KMA considers TCTS and storm age relatively less than other agencies.

To determine the range in which the wind radius differences between the three agencies were large for V_{\max} , latitude, TCTS, and storm age, the mean wind radii and their standard deviations were compared by dividing the parameters into bins at intervals of 10 kts, 5° , 2 m s^{-1} , and 1 day,

respectively. The spacing of bins were determined such that the sample size of each bin was sufficient for statistical analysis. In terms of Vmax (Fig. 6a and e), R30 and R50 tended to increase as Vmax increased in all agencies' estimations. Specifically, the RSMC Tokyo had the largest R30 values in all bins, followed by the KMA and JTWC. For R50, the RSMC Tokyo also had the largest values in all bins, followed by the JTWC and KMA. The order, by agency, for R30 and R50 is also generally similar for latitude, TCTS, and storm age (Fig. 6b–d and f–h).

Regarding latitude (Fig. 6b and f), R30 and R50 tended to increase as the latitude increased in the RSMC Tokyo and JTWC estimates but did not change significantly in the KMA estimates. These results are consistent with the finding that the TC wind radii in the KMA estimates did not correlate with latitude. Because of this tendency, the KMA's estimates of wind radii at low latitudes were similar to those of other agencies, but the differences gradually increased at higher latitudes. The TCTS trends were similar to the latitude trends (Fig. 6c and g). This is because the TCTS correlates strongly with latitude, increasing with higher latitudes. For storm age, as it increases, R30 and R50 tended to increase in all agencies (Fig. 6d and h), which can be explained by the fact that storm age is significantly correlated with both Vmax and latitude. In particular, for a high storm ages of

more than 6 days, it is more similar to the trend of latitude than Vmax.

3.3 Asymmetrical Characteristics

The asymmetries in wind radii estimated by the three agencies were investigated, and the ways in which they were related to Vmax, latitude, TCTS, and storm age in each agency's estimations were specifically examined. First, a comparison of the mean R30 asymmetry values between the agencies showed that the KMA had the smallest value (29.7 km), followed by the JTWC (43.6 km) and RSMC Tokyo (48.6 km) (Table 3). For the normalized asymmetries, the order was changed—the smallest KMA (0.14) and RSMC Tokyo (0.14), followed by JTWC (0.21). In terms

Table 3 Same as in Table 1, but for mean asymmetry of tropical cyclone wind radii. Normalized values are shown in parentheses

Mean Asymmetry	KMA	RSMC Tokyo	JTWC
R30	29.7 ± 10.8 km	48.6 ± 47.3 km	43.6 ± 31.1 km
(Normalized)	(0.14 ± 0.06)	(0.14 ± 0.13)	(0.21 ± 0.15)
R50	11.5 ± 5.7 km	4.7 ± 13.3 km	21.5 ± 15.7 km
(Normalized)	(0.13 ± 0.07)	(0.04 ± 0.09)	(0.19 ± 0.12)

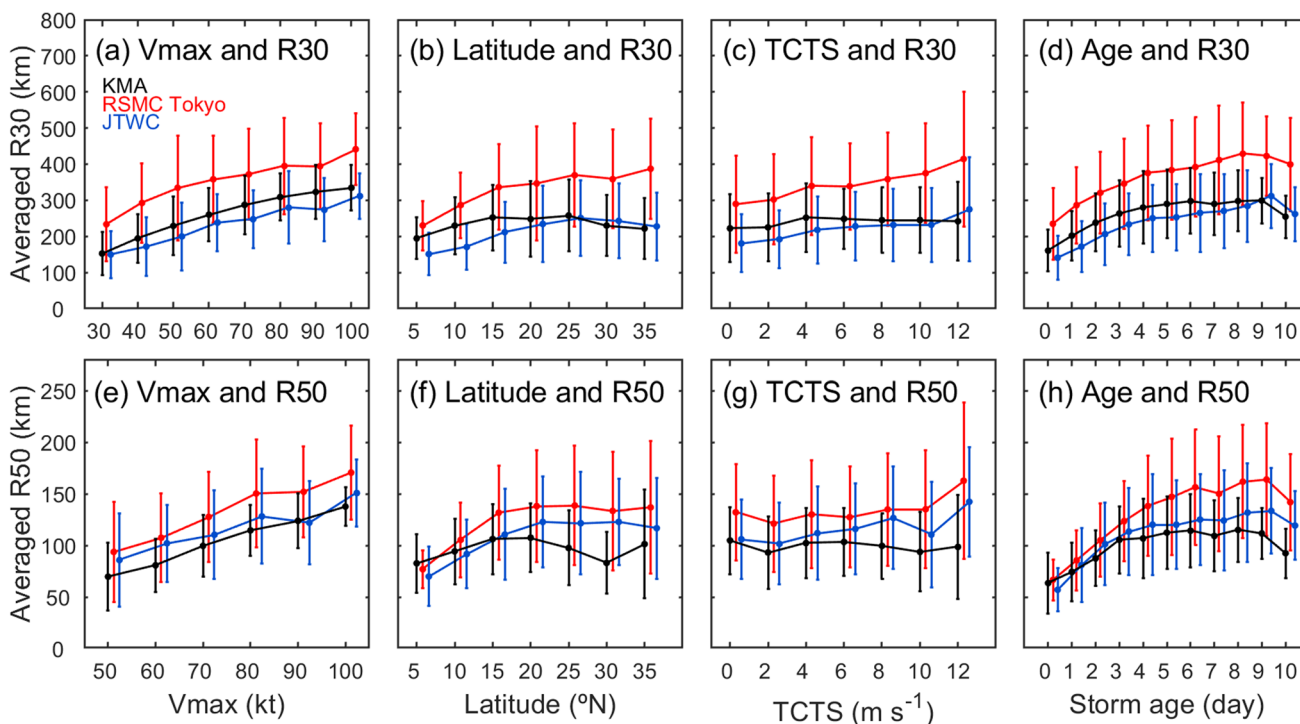


Fig. 6 Comparison of the mean values (circles) and standard deviations (error bars) in each bin of maximum wind speed (Vmax) (a, e), latitude (b, f), TC translation speed (TCTS) (c, g), and storm age (Age) (d, h) for R30 (top panels) and R50 (bottom panels) estimates

of the KMA (black), RSMC Tokyo (red), and JTWC (blue). The bins are divided into intervals of 10 kts, 5°N, 2 m s⁻¹, and 1 day for Vmax, latitude, TCTS, and storm age, respectively

of the spatial distributions of the asymmetries (Fig. 7a–c), the KMA showed uniform distributions with relatively small values (20–40 km) in most regions, while the RSMC Tokyo and JTWC showed significant regional variations, with large (small) values in the eastern seas of Japan and near the KP (South China seas and tropical seas). The regional

differences in the estimated asymmetries between the agencies depended on how each agency considered the factors affecting them. A comparison of the mean R30 asymmetries related to Vmax, latitude, TCTS, and storm age in each agency's estimations is shown in Fig. 8a–d. The RSMC Tokyo and JTWC showed a tendency toward increased asymmetries

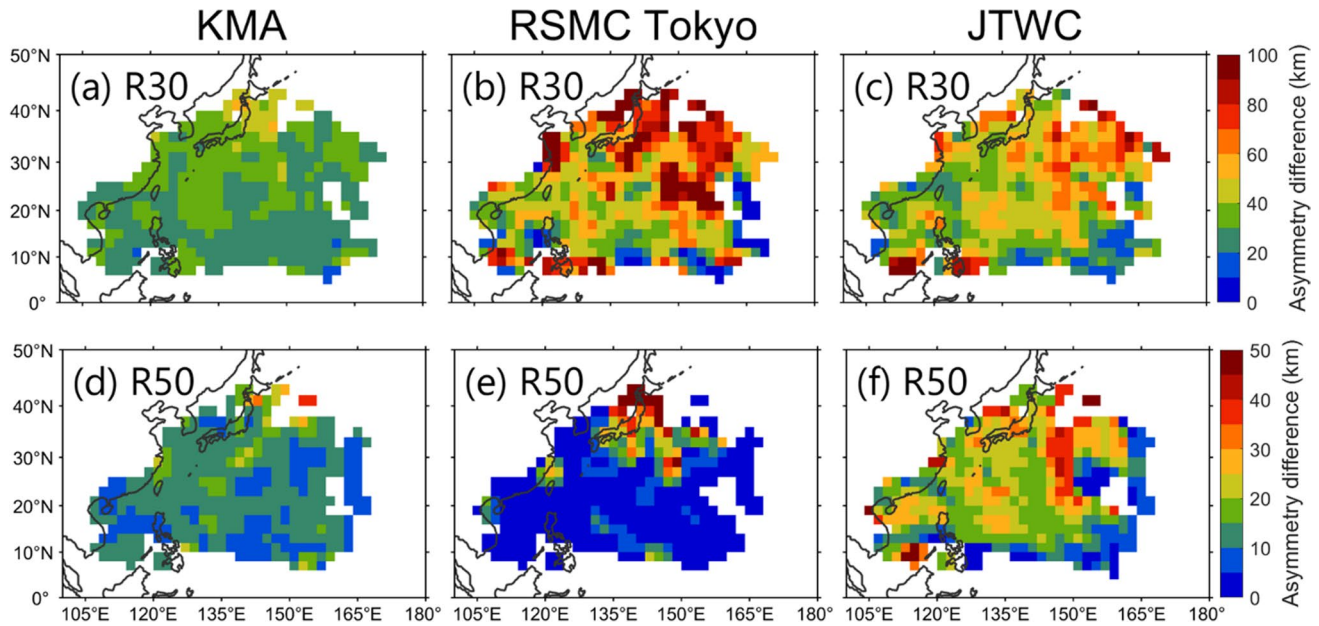


Fig. 7 Same as in Fig. 3, but for mean asymmetry values of tropical cyclone wind radii

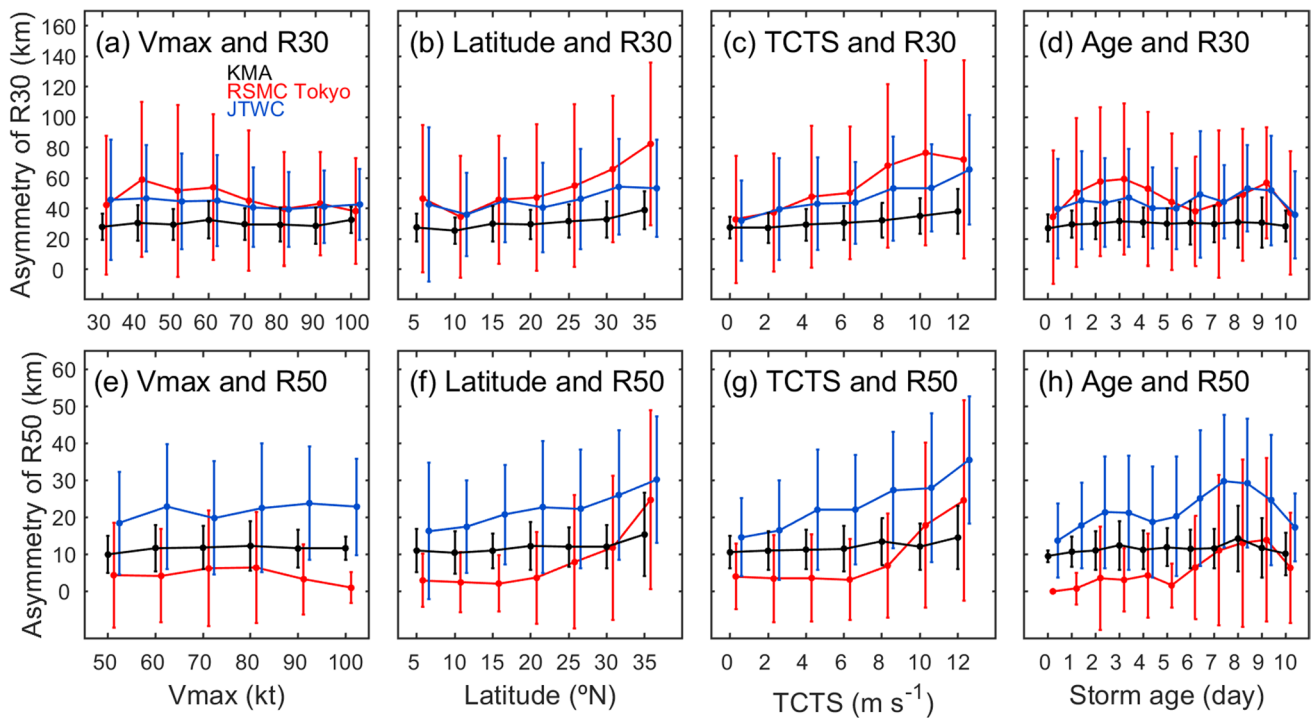


Fig. 8 Same as in Fig. 6, but for mean asymmetry values of tropical cyclone wind radii

as the latitude and STS increased, whereas the KMA estimates did not depend on the latitude or the STS.

For R50's asymmetry, mean and normalized values were the smallest in the RSMC Tokyo (4.7 km and 0.04) and the greatest in the JTWC (21.5 km and 0.19) (Table 3). In normalized comparisons, the JTWC estimates show, on average, the greatest asymmetries for both R30 and R50. On the other hand, the RSMC Tokyo showed almost zero asymmetries for R50 in most regions, except for the eastern seas of Japan (Fig. 7b and e), while the KMA and JTWC showed similar patterns in the spatial distributions of R30 and R50 (Fig. 7a, c, d, and f). This suggests that the KMA and JTWC used similar techniques for R30 and R50 estimations, whereas the RSMC Tokyo seems to have used a different method for each. In R50, the JTWC heavily relied on the latitude and TCTS, whereas the KMA hardly relied on these variables (Fig. 8e–h). The RSMC Tokyo showed constant and weak asymmetries at low latitudes (below 20°) and at slow TCTSs (below 6 m s⁻¹), but the asymmetries tended to increase rapidly at higher latitudes and at faster TCTSs (more than 8 m s⁻¹; Fig. 8f–g). For storm age, the JTWC and RSMC Tokyo showed a similar pattern of asymmetry increasing with storm age up to 8–9 days, but decreasing thereafter, whereas the KMA did not depend on storm age (Fig. 8e–h). On the other hand, Vmax did not influence the asymmetries for either R30 or R50 in any agency's estimations (Fig. 8a and e).

3.4 Case Studies Comparing TC Wind Radius Estimates

The TC cases that showed significant differences in mean values and asymmetries in wind radii estimates between the three agencies (reported in the previous section) were selected to investigate the respective wind radius estimation characteristics. The first case was Typhoon Jebi (2018), which showed a large difference in mean R30 between the RSMC Tokyo and the other two agencies (Figs. 9 and 10). Around 00:00 UTC on August 31, when Jebi had the strongest intensity (gray line in Fig. 9), the mean R30 values of the three agencies were similar. Subsequently, as Jebi weakened, the difference between the RSMC Tokyo and KMA/JTWC gradually increased, reaching over 500 km at the decay stage of the typhoon (12:00 UTC on September 4; red, blue, and green lines in Fig. 9). Interestingly, the RSMC Tokyo, unlike the KMA and JTWC, estimated a sharp increase in R30 as Jebi rapidly weakened.

To examine why the RSMC Tokyo estimated a significantly larger R30 value than the other two agencies during the rapid weakening stage, we compared the R30 values of the three agencies with a 1000-hPa wind field from the Global Forecast System (GFS) analysis data (Fig. 10). The model-estimated mean R30 (MM-R30, solid black lines)

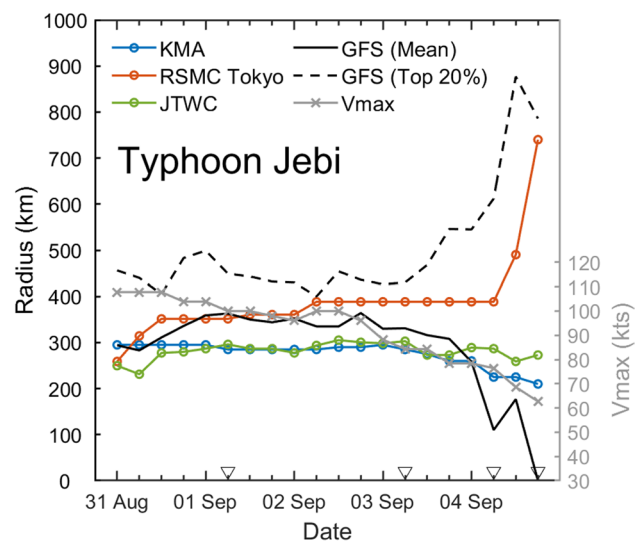


Fig. 9 Comparison of mean R30 value estimates of the KMA (blue), RSMC Tokyo (red), and JTWC (green) with the mean (solid black line) and top 20% (dashed black line) R30 values estimated from GFS winds at 1000 hPa for Typhoon Jebi (2018) from 00:00 UTC on August 31 to 18:00 UTC on September 12 at 6-h intervals. The solid gray line represents the maximum wind speed (Vmax) estimated by the RSMC Tokyo. The triangles indicate the times of the spatial distributions presented in Fig. 11

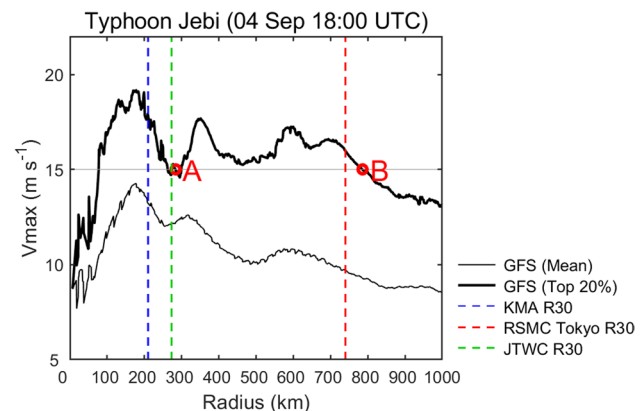


Fig. 10 Mean radial wind profiles of 1000-hPa GFS wind at 18:00 UTC on September 4 when Typhoon Jebi (2018) rapidly weakened. Thin and thick black lines indicate mean and top-20% mean values, respectively. Blue, red, and green dashed lines indicate R30s estimated from the KMA, RSMC Tokyo, and JTWC, respectively. Points A and B are where Vmax is 15 m s⁻¹. At 18:00 UTC on September 4, all mean radial winds (thin black line) were less than 15 m s⁻¹, which explains why the model-estimated mean R30 was zero in Fig. 9

decreased as Jebi weakened, as in the KMA and JTWC estimates, whereas the model-estimated mean R30 in the top 20% (M20-R30, dashed black line) increased sharply, as in the RSMC Tokyo estimate. In fact, at 18:00 UTC on September 4, when the difference between MM-R30 and M20-R30 was the largest, the radial wind profile of the top 20%

was 15 m s^{-1} at two points—A (284 km) and B (786 km) (Fig. 10). These are candidates that can be estimated to be R30. Interestingly, at this time, KMA and JTWC estimated the value near A as R30 (blue and green dashed line in Fig. 10) and RSMC Tokyo estimated the value near B as R30 (red dashed line). This suggests that when determining R30, the RSMC Tokyo included a wide area of gale-force winds, far from the TC center, induced by an extratropical transition of the TC, mid-latitude pressure system, and topography.

This characteristic was evident when the spatial distributions of model winds with R30 were compared between the three agencies (Fig. 11). At 06:00 UTC on September 1 and 3, when Jebi was in the open ocean, the model's wind field was symmetrical, and the model-estimated R30 was similar to that estimated by the three agencies (Fig. 11a–b). However, at 06:00 UTC on September 4, when Jebi made landfall in Japan, the strong wind area at the storm center disappeared, and an asymmetrical strong wind region appeared outside the TC, mostly on the ocean side (Fig. 11c). At 18:00 UTC on September 4, when Jebi weakened further, strong wind regions were distributed from the southern to the northern tip of Japan, far from the TC center (Fig. 11d), which is related to the low pressure system that existed before Jebi made landfall (Anh et al. 2019). At that time, the RSMC Tokyo estimated the R30 to be as large as 740 km,

including most of the strong wind region outside the TC, while the KMA and JTWC estimated it to be 210 km and 273 km, respectively, considering only weakened winds near the storm (Fig. 11d). This is attributed to differences in the three agencies' policies for defining gale-force TC winds. Specifically, the RSMC Tokyo considers the gale-force wind radius to include areas where strong winds occur, even if they are far from the storm's center, mainly for damage and disaster prevention purposes. On the other hand, the KMA and JTWC seem to determine the gale-force wind radius by focusing on the strong wind area of the TC itself.

To further explore the characteristics of the asymmetry differences between the three agencies, Typhoon Soulik (2018) was used in another case study. Overall, the KMA showed a small asymmetry (20–40 km) with no significant change over Soulik's lifetime, while the RSMC Tokyo and JTWC showed significant variations (0–83 and 10–90 km, respectively), similar to the variations in the TCTS (Fig. 12a and b), with the asymmetry increasing and decreasing as the TCTS increased and decreased. In line with the results obtained from the previously mentioned correlation analysis (Table 3; Fig. 8c), this result suggests that the KMA does not consider the TCTS when estimating wind radii.

A comparison of the spatial distribution of the model wind with the best-track R30 illustrated the characteristics of the agency-dependent asymmetries (Fig. 13). First, in the

Fig. 11 Comparison of R30 (gray contour) estimated from the GFS winds (shade) at 1000 hPa with the mean R30 values estimated by the RSMC Tokyo (red circle), KMA (blue circle), and JTWC (green circle) for Typhoon Jebi (2018) at 06:00 UTC on September 1 (a), 06:00 UTC on September 3, 06:00 UTC on September 4 (c), and 18:00 UTC on September 4 (d). The red crosses indicate the tropical cyclone's center. The maximum wind speed (V_{\max}) estimated by the RSMC Tokyo and the mean R30 values of the three agencies are shown in each panel

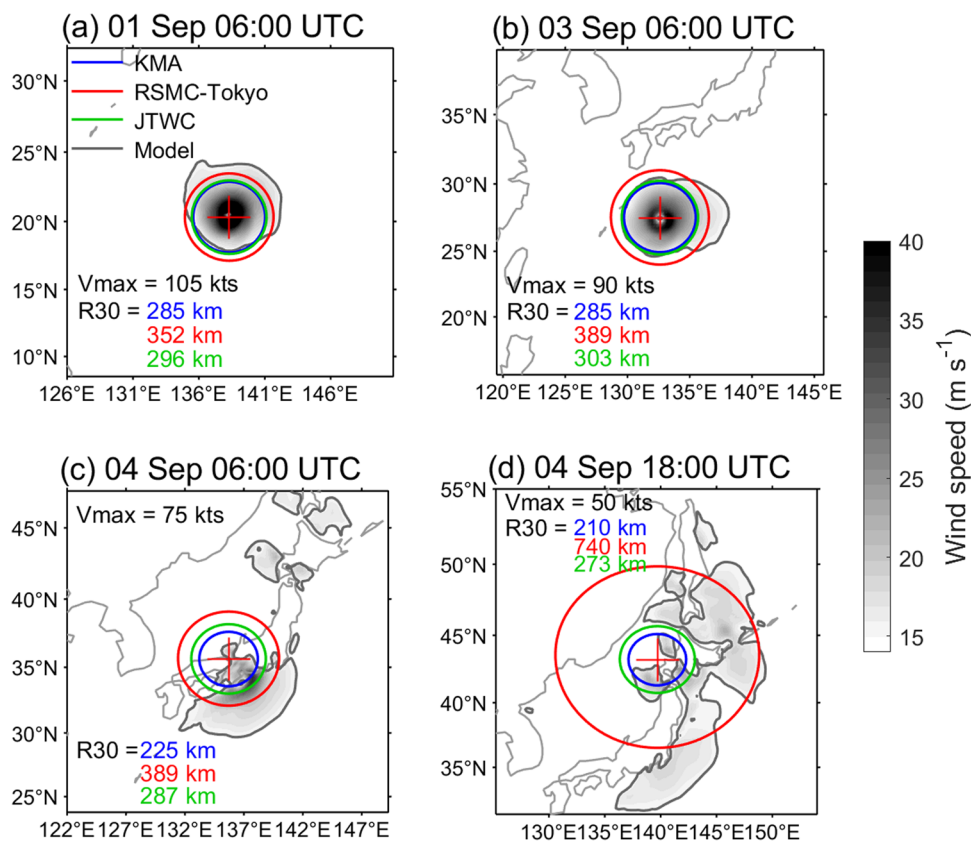
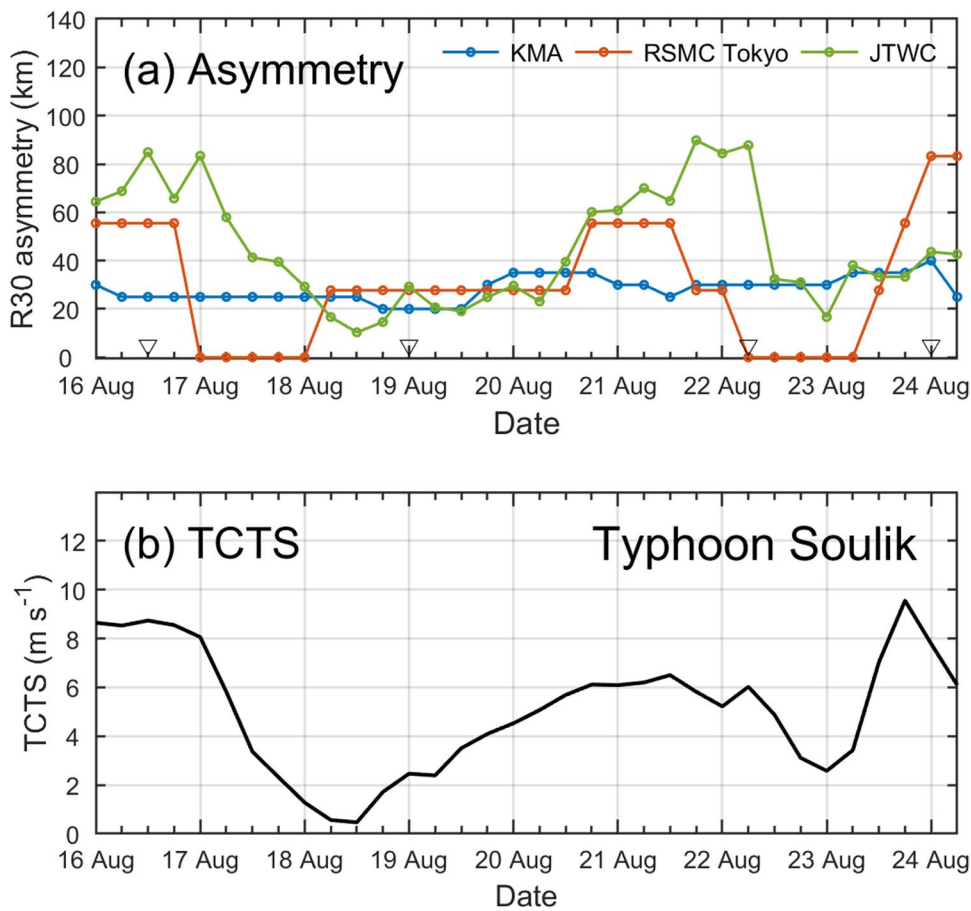


Fig. 12 Comparison of the R30 asymmetries (a) estimated by the KMA (blue), RSMC Tokyo (red), and JTWC (green) with the TC translation speed (TCTS) (b) for Typhoon Soulik (2018) from 00:00 UTC on August 16 to 06:00 UTC on August 24 at 6-h intervals. The triangles represent the times of the spatial distributions presented in Fig. 13



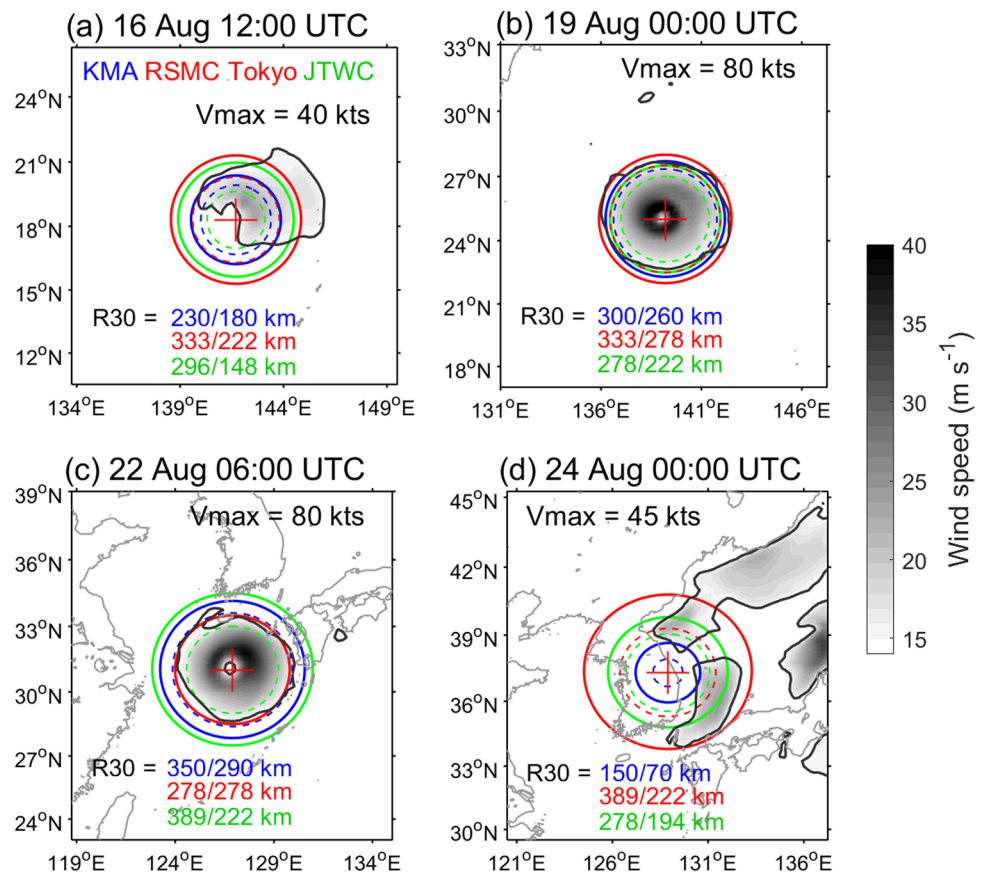
early stages of TC development at 12:00 UTC on August 16 (Fig. 13a), the model winds showed a clear asymmetrical distribution, which seems to have been related to the relatively fast TCTS (8.7 m s^{-1}). At that time, the RSMC Tokyo and JTWC showed a significant difference between the longest and shortest radii, whereas the KMA showed a relatively small difference (compare the solid and dashed lines or the values in Fig. 13a). At 00:00 UTC on August 19, when the TC was moving slowly (2.5 m s^{-1}) and increasing in intensity, the model-estimated R30 showed a nearly symmetrical distribution with small differences between the longest and shortest radii in the three agencies' estimates (Fig. 13b). At 06:00 UTC on August 22, the model wind and RSMC Tokyo's R30 were relatively symmetrical, while those of the KMA and JTWC were asymmetrical (Fig. 13c). Finally, at 00:00 UTC on August 24, when the TC made landfall over the KP and began to decay, the model wind was particularly asymmetrical (Fig. 13d), with the gale-force winds more widely distributed outside the northeast than near the TC center. At that time, considering the weakening of the TC, the JTWC and KMA estimated both the longest and shortest radii to be small, while the RSMC Tokyo estimated the longest radius to be very large by including strong wind areas outside the TC, which resulted in a significant asymmetry.

In summary, the KMA considers weak asymmetries—greater than the RSMC Tokyo estimates and smaller than the JTWC estimates—which do not change significantly during the lifetimes of TCs. The JTWC estimates the wind radius, on average, most asymmetrical, with significant variations according to the latitude and TCTS. The RSMC Tokyo tends to estimate the wind radius completely symmetrically before TCs approach higher latitudes (around 20°N) and highly asymmetrical thereafter. Again, this is because the RSMC Tokyo estimates gale-force wind radii, including areas where strong winds occur, even if they are far from the storm's center, for damage and disaster prevention purposes.

4 Discussion and Conclusion

TC wind radii, which constitute some of the most important information for predicting disasters caused by TCs, have been provided by the KMA, RSMC Tokyo, and JTWC since 2015. However, the detailed characteristics of the wind radii estimated by each agency have hitherto not been investigated. This study compared the mean values and asymmetries in the three data sets of TC wind radii (R30 and R50) in the western North Pacific between 2015

Fig. 13 Comparison of R30 (gray contours) estimated from the GFS winds (shade) at 1000 hPa with the longest and shortest R30 values estimated by the RSMC Tokyo (red circle), KMA (blue circle), and JTWC (green circle) for Typhoon Soulik (2018) at 12:00 UTC on August 16 (a), 00:00 UTC on August 19 (b), 06:00 UTC on August 22 (c), and 00:00 UTC on August 24 (d). The solid and dashed circles indicate the longest and shortest R30. The red crosses indicate the tropical cyclone's center. The maximum wind speed (V_{max}) estimated by the RSMC Tokyo and the longest and shortest R30 of the three agencies are shown in each panel



and 2018 and explored the factors that each agency mainly considers when estimating wind radii.

First, a comparison between the mean values both R30 and R50 of the three agencies showed that the RSMC Tokyo had the largest mean value—about 91 and 118 km for R30 (about 29 and 17 km for R50) larger than the mean values of the KMA and JTWC, respectively (Table 1). The differences increased as the mean wind radii and latitude increased (Figs. 2 and 6b and f). A correlation analysis revealed that the KMA considered only V_{max} when estimating TC wind radii, while the RSMC Tokyo and JTWC considered not only V_{max} but also the latitude and TCTS partially (Table 2).

Differences in wind radius between the three agencies were also found in the estimated asymmetries, defined as the differences between the longest and shortest wind radii (Table 3). The KMA showed the smallest mean asymmetry (29.7 km) for R30, which was uniformly distributed within 20–40 km in most regions. The RSMC Tokyo and JTWC showed greater mean asymmetries (48.6 and 43.6 km, respectively) than the KMA, with considerable regional variations. The mean asymmetry for R50 was smallest in the RSMC Tokyo estimates (4.7 km) and greatest in the JTWC estimates (21.5 km). The asymmetries in the RSMC Tokyo and JTWC estimates tended to increase with the latitude and

TCTS, whereas the KMA did not rely on these parameters, thus estimating locally uniform wind radii.

Through two case studies (Typhoons Jebi and Soulik in 2018), we confirmed the different characteristics of the wind radius estimations of the three agencies. When determining R30, RSMC Tokyo includes a wide area of gale-force winds, far from the TC center, induced by an extratropical transition of the TC, mid-latitude pressure system, and topography. This increases the estimated longest wind radius, especially at higher latitudes (above 20°N), which in turn increases the mean wind radius and asymmetry in the RSMC Tokyo data. On the other hand, the KMA and JTWC generally estimate the TC wind radius by focusing on the strong wind area of the TC itself, which explains why their mean R30 and asymmetries are on average smaller than those of the RSMC Tokyo.

This study provides quantitative information on the characteristics of and differences in gale-force and storm-force wind radii between the three agencies. We found that the wind radii in best track data differ significantly between the three agencies not only in mean values but also in asymmetrical characteristics and spatial distributions. These differences are primarily due to agency-specific policies defining the wind radius and determining whether the estimations should focus on the TC itself or include the wind

outside the TC for damage and disaster prevention purposes. At this point, it is impossible to conclude which policy is the best or which wind radius estimation method is the most reliable because each agency's policy has been established for its own purposes. However, it is clear that due to these policy differences, the TC radius data are too uncertain and inconsistent to be used in research, although previous studies have found that the wind radii in best track data constitute sufficiently reliable information (Knaff et al. 2016; Dolling et al. 2016). Therefore, it is essential for researchers to know in advance the characteristics of the wind radius estimations of each agency and to select and use the data according to each study's purpose. This study provides useful information for making the appropriate selection. The results can also be used as the basis for developing a method for consistent wind radius estimations by various agencies.

Acknowledgements This research was supported by the project titled "Development of typhoon analysis and forecast technology (KMA2018-00722)" of the National Typhoon Center at the Korea Meteorological Administration, the project titled "Construction of Ocean Research Stations and their Application Studies" funded by the Ministry of Oceans and Fisheries, and Basic Science Research Program through the National Research Foundation of Korea (NRF) funded by the Ministry of Education (2021R1A2C1005287).

Declarations

Conflict of Interest The authors declare that they have no conflict of interest.

Open Access This article is licensed under a Creative Commons Attribution 4.0 International License, which permits use, sharing, adaptation, distribution and reproduction in any medium or format, as long as you give appropriate credit to the original author(s) and the source, provide a link to the Creative Commons licence, and indicate if changes were made. The images or other third party material in this article are included in the article's Creative Commons licence, unless indicated otherwise in a credit line to the material. If material is not included in the article's Creative Commons licence and your intended use is not permitted by statutory regulation or exceeds the permitted use, you will need to obtain permission directly from the copyright holder. To view a copy of this licence, visit <http://creativecommons.org/licenses/by/4.0/>.

References

- Anh, L.T., Takagi, H., Heidarzadeh, M., Takata, Y., Takahashi, A.: Field surveys and numerical simulation of the 2018 typhoon Jebi: impact of high waves and storm surge in semi-enclosed Osaka bay. *Japan. Pure. Appl. Geophys.* **176**, 4139–4160 (2019). <https://doi.org/10.1007/s00024-019-02295-0>
- Barcikowska, M., Feser, F., Von Storch, H.: Usability of best track data in climate statistics in the western North Pacific. *Mon. Weather Rev.* **140**, 2818–2830 (2012). <https://doi.org/10.1175/MWR-D-11-00175.1>
- Bell, K., Ray, P.S.: North Atlantic hurricanes 1977–99: surface hurricane-force wind radii. *Mon. Weather Rev.* **132**, 1167–1189 (2004). [https://doi.org/10.1175/1520-0493\(2004\)132<1167:NAHSHW>2.0.CO;2](https://doi.org/10.1175/1520-0493(2004)132<1167:NAHSHW>2.0.CO;2)
- Bentamy, A., Croize-Fillon, D., Perigaud, C.: Characterization of ASCAT measurements based on buoy and QuikSCAT wind vector observations. *Ocean Sci.* **4**, 265–274 (2008). <https://doi.org/10.5194/os-4-265-2008>
- Brennan, M.J., Hennon, C.C., Knabb, R.D.: The operational use of QuikSCAT Ocean surface vector winds at the National Hurricane Center. *Weather Forecast.* **24**, 621–645 (2009). <https://doi.org/10.1175/2008WAF2222188.1>
- Cha, E.J., Knutson, T.R., Lee, T.C., Ying, M., Nakaegawa, T.: Third assessment on impacts of climate change on tropical cyclones in the typhoon committee region—part II: future projections. *Trop. Cyclone Res. Rev.* **9**, 75–86 (2020). <https://doi.org/10.1016/j.tcr.2020.04.005>
- Chan, K.T., Chan, J.C.: Size and strength of tropical cyclones as inferred from QuikSCAT data. *Mon. Weather Rev.* **140**, 811–824 (2012). <https://doi.org/10.1175/MWR-D-10-05062.1>
- Chan, K.T., Chan, J.C.: Angular momentum transports and synoptic flow patterns associated with tropical cyclone size change. *Mon. Weather Rev.* **141**, 3985–4007 (2013). <https://doi.org/10.1175/MWR-D-12-00204.1>
- Chavas, D.R., Lin, N., Emanuel, K.: A model for the complete radial structure of the tropical cyclone wind field. Part I: comparison with observed structure. *J. Atmos. Sci.* **72**, 3647–3662 (2015). <https://doi.org/10.1175/JAS-D-15-0014.1>
- DeMaria, M., Pickle, J.D.: A simplified system of equations for simulation of tropical cyclones. *J. Atmos. Sci.* **45**, 1542–1554 (1988). [https://doi.org/10.1175/1520-0469\(1988\)045<1542:ASSOEF>2.0.CO;2](https://doi.org/10.1175/1520-0469(1988)045<1542:ASSOEF>2.0.CO;2)
- Dolling, K., Ritchie, E.A., Tyo, J.S.: The use of the deviation angle variance technique on geostationary satellite imagery to estimate tropical cyclone size parameters. *Weather Forecast.* **31**, 1625–1642 (2016). <https://doi.org/10.1175/WAF-D-16-0056.1>
- Dougherty, E., Davis, C.A.: Observations of Wind Asymmetries in Atlantic Tropical Cyclones. In 2014 AGU Fall Meeting. AGU (2014)
- Frank, W.M., Gray, W.M.: Radius and frequency of 15 m s⁻¹ (30 kt) winds around tropical cyclones. *J. Appl. Meteorol.* **19**, 219–223 (1980). [https://doi.org/10.1175/1520-0450\(1980\)019<0219:RAFOMS>2.0.CO;2](https://doi.org/10.1175/1520-0450(1980)019<0219:RAFOMS>2.0.CO;2)
- Hong, S., Shin, I.: Wind speed retrieval based on sea surface roughness measurements from spaceborne microwave radiometers. *J. Appl. Meteorol. Clim.* **52**, 507–516 (2013). <https://doi.org/10.1175/JAMC-D-11-0209.1>
- Kimball, S.K., Mulekar, M.S.: A 15-year climatology of North Atlantic tropical cyclones. Part I: Size parameters. *J. Climate.* **17**, 3555–3575 (2004). [https://doi.org/10.1175/1520-0442\(2004\)017<3555:AYCONA>2.0.CO;2](https://doi.org/10.1175/1520-0442(2004)017<3555:AYCONA>2.0.CO;2)
- KMA: Typhoon Best Track, Korea Meteorological Administration, 3pp (2019). https://www.kma.go.kr/download_01/typhoon/typbesttrack_2019.pdf (in Korean)
- Knaff, J.A., Sampson, C.R., DeMaria, M., Marchok, T.P., Gross, J.M., McAdie, C.J.: Statistical tropical cyclone wind radii prediction using climatology and persistence. *Weather Forecast.* **22**, 781–791 (2007). <https://doi.org/10.1175/WAF1026.1>
- Knaff, J.A., DeMaria, M., Molenaar, D.A., Sampson, C.R., Seybold, M.G.: An automated, objective, multiple-satellite-platform tropical cyclone surface wind analysis. *J. Appl. Meteorol. Clim.* **50**, 2149–2166 (2011). <https://doi.org/10.1175/2011JAMC2673.1>
- Knaff, J.A., Slocum, C.J., Musgrave, K.D., Sampson, C.R., Strahl, B.R.: Using routinely available information to estimate tropical cyclone wind structure. *Mon. Weather Rev.* **144**, 1233–1247 (2016). <https://doi.org/10.1175/MWR-D-15-0267.1>
- Knaff, J.A., Sampson, C.R., Chirokova, G.: A global statistical-dynamical tropical cyclone wind radii forecast scheme.

- Weather Forecast. **32**, 629–644 (2017). <https://doi.org/10.1175/WAF-D-16-0168.1>
- Knaff, J.A., et al.: Estimating tropical cyclone surface winds: current status, emerging technologies, historical evolution, and a look to the future. *Trop. Cyclone Res. Rev.* **10**, 125–150 (2021). <https://doi.org/10.1016/j.tcr.2021.09.002>
- Kossin, J.P., et al.: Estimating hurricane wind structure in the absence of aircraft reconnaissance. *Weather Forecast.* **22**, 89–101 (2007). <https://doi.org/10.1175/WAF985.1>
- Kwon, M.: Estimation and statistical characteristics of the radius of maximum wind of tropical cyclones using COMS IR imagery. *Atmosphere.* **22**, 473–481 (2012). <https://doi.org/10.14191/Atmos.2012.22.4.473> (in Korean with English abstract)
- Landsea, C.W., Franklin, J.L.: Atlantic hurricane database uncertainty and presentation of a new database format. *Mon. Weather Rev.* **141**, 3576–3592 (2013). <https://doi.org/10.1175/MWR-D-12-00254.1>
- Lee, Y.K., Kwon, M.: An estimation of the of tropical cyclone size using COMS infrared imagery. *Atmosphere.* **25**, 569–573 (2015). <https://doi.org/10.14191/Atmos.2015.25.3.569> (in Korean with English abstract)
- Lee, C.S., Cheung, K.K., Fang, W.T., Elsberry, R.L.: Initial maintenance of tropical cyclone size in the western North Pacific. *Mon. Weather Rev.* **138**, 3207–3223 (2010). <https://doi.org/10.1175/2010MWR3023.1>
- Lungu, T., Callahan, P.S.: QuikSCAT science data product user's manual: Overview and geophysical data products. D-18053-Rev A, version, 3 (2006)
- McAdie, C.J.: Development of a wind-radii CLIPER model. Preprints, 24th Conf. on Hurricanes and Tropical Meteorology, Miami, FL, Amer. Meteor. Soc. **5**, 170–171 (2004)
- Merrill, R.T.: A comparison of large and small tropical cyclones. *Mon. Weather Rev.* **112**, 1408–1418 (1984). [https://doi.org/10.1175/1520-0493\(1984\)112<1408:ACOLAS>2.0.CO;2](https://doi.org/10.1175/1520-0493(1984)112<1408:ACOLAS>2.0.CO;2)
- Misra, T., et al.: SCATSAT-1 Scatterometer: an improved successor of OSCAT. *Curr. Sci.* **117**, 941–949 (2019). <https://doi.org/10.18520/cs/v117/i6/941-949>
- Muroi, C.: Brief history and recent activities of RSMC Tokyo-typhoon Centre. *Trop. Cyclone Res. Rev.* **7**, 57–64 (2018). <https://doi.org/10.6057/2018TCRR01.09>
- Sampson, C.R., Knaff, J.A.: A consensus forecast for tropical cyclone gale wind radii. *Weather Forecast.* **30**, 1397–1403 (2015). <https://doi.org/10.1175/WAF-D-15-0009.1>
- Sampson, C.R., Fukada, E.M., Knaff, J.A., Strahl, B.R., Brennan, M.J., Marchok, T.: Tropical cyclone gale wind radii estimates for the western North Pacific. *Weather Forecast.* **32**, 1029–1040 (2017). <https://doi.org/10.1175/WAF-D-16-0196.1>
- Sampson, C.R., Goerss, J.S., Knaff, J.A., Strahl, B.R., Fukada, E.M., Serra, E.A.: Tropical cyclone gale wind radii estimates, forecasts, and error forecasts for the western North Pacific. *Weather Forecast.* **33**, 1081–1092 (2018). <https://doi.org/10.1175/WAF-D-17-0153.1>
- Schenkel, B.A., Lin, N., Chavas, D., Oppenheimer, M., Brammer, A.: Evaluating outer tropical cyclone size in reanalysis datasets using QuikSCAT data. *J. Clim.* **30**, 8745–8762 (2017). <https://doi.org/10.1175/JCLI-D-17-0122.1>
- Song, J., Klotzbach, P.J.: Wind structure discrepancies between two best track datasets for western North Pacific tropical cyclones. *Mon. Weather Rev.* **144**, 4533–4551 (2016). <https://doi.org/10.1175/MWR-D-16-0163.1>
- Weatherford, C.L., Gray, W.M.: Typhoon structure as revealed by aircraft reconnaissance. Part I: data analysis and climatology. *Mon. Weather Rev.* **116**, 1032–1043 (1988). [https://doi.org/10.1175/1520-0493\(1988\)116<1032:TSARBA>2.0.CO;2](https://doi.org/10.1175/1520-0493(1988)116<1032:TSARBA>2.0.CO;2)
- Wu, L., Tian, W., Liu, Q., Cao, J., Knaff, J.A.: Implications of the observed relationship between tropical cyclone size and intensity over the western North Pacific. *J. Clim.* **28**, 9501–9506 (2015). <https://doi.org/10.1175/JCLI-D-15-0628.1>
- Xu, J., Wang, Y.: Dependence of tropical cyclone intensification rate on sea surface temperature, storm intensity, and size in the western North Pacific. *Weather Forecast.*, **33**, 523–537 (2018). <https://doi.org/10.1175/WAF-D-17-0095.1>
- Zhao, K., Zhao, C.: Evaluation of HY-2A scatterometer ocean surface wind data during 2012–2018. *Remote Sens.* **11**, 2968 (2019). <https://doi.org/10.3390/rs11242968>

Publisher's Note Springer Nature remains neutral with regard to jurisdictional claims in published maps and institutional affiliations.